

Scanning tunneling microscopy investigation of atomic-scale carbon nanotube defects produced by Ar⁺ ion irradiation

Z. Osváth*, G. Vértesy, L. Tapasztó, F. Wéber, Z.E. Horváth, J. Gyulai, L.P. Biró

Research Institute for Technical Physics and Materials, Sciences (MFA), H-1525 Budapest, P.O. Box 49, Hungary

Available online 2 November 2005

Abstract

Multi-wall carbon nanotubes (MWCNTs) dispersed on graphite (HOPG) substrate were irradiated with Ar⁺ ions of 30 keV, using a dose of $D=5 \times 10^{11}$ ions/cm². The irradiated nanotubes were investigated by scanning tunneling microscopy (STM) and spectroscopy (STS) under ambient conditions. Atomic resolution STM images revealed individual nanotube defects, which appeared as “hillocks” of 0.1–0.2 nm in height, due to the locally changed electronic structure. The results are in agreement with previous theoretical predictions. Electron density patterns (superstructures) were observed near the defect sites, which originated from the interference of incident waves and waves scattered by defects. The period of these superstructures is larger than the period determined by the atomic structure. After annealing at 450 °C in nitrogen atmosphere, the irradiated MWCNTs were investigated again. The effect of heat treatment on the irradiation-induced nanotube-defects was observed both on the STM images and on the recorded STS spectra.

© 2005 Elsevier B.V. All rights reserved.

Keywords: STM; STS; Carbon nanotube; Defects; Irradiation

1. Introduction

The carbon nanotubes (CNTs) regarded as perfect cylinders made from sheets of graphite [1] often contain various kinds of defects in their structure. Defects like non-hexagonal carbon rings are responsible for the formation of nanotube junctions [2] and branched nanotubes [3,4], while the presence of vacancy-related defects or local deformations in straight nanotubes can influence their transport properties [5]. Nanotube defects can form during the synthesis or can be introduced for example by purification treatment or irradiation with charged particles. Experiments show that both electron and heavy ion irradiation can modify the structure and dimensions of CNTs [6,7]. Zhu et al. [8] pointed out that energetic Ar⁺ ions produce dangling bonds (vacancies) on the surface of nanotubes. A brief overview on the irradiation-induced effects in carbon nanotubes has been given recently [9]. Even more recently, atomic-scale carbon nanotube defects were successfully observed by HRTEM [10].

The STM signatures of topological CNT defects were also simulated [11,12]. Krasheninnikov et al. predicted the STM

images of individual vacancies in single wall CNTs using tight-binding calculations [13,14]. They demonstrated that different type of vacancy-related defects have different signatures in the STM images [15].

In the present work we report experimental atomic resolution STM images of individual carbon nanotube defects created by irradiation.

2. Experimental

In this experiment we used MWCNTs grown by the arc-discharge method. A suspension was prepared by sonicating 1 mg of CNT sample in 20 ml of toluene for 60 min. Droplets of this suspension were dispersed on a cleaved HOPG substrate. After the deposition of the CNTs the sample was introduced in an ion implanter and was irradiated with Ar⁺ ions of 30 keV using a low dose of $D=5 \times 10^{11}$ ions/cm². The ion current was $I=0.9 \mu\text{A}$, and the irradiation was done at normal incidence. The low dose was used in order to create individual, non-overlapping defects in the nanotube walls. The irradiated sample was investigated by STM (constant current mode) and STS. These measurements were done with a Nanoscope E instrument operating under ambient conditions, with tunneling currents (I_t) of 0.3–1 nA and bias voltages (U_t) in the range of

* Corresponding author. Tel.: +36 1 392 2222x1157; fax: +36 1 392 2226.
E-mail address: osvath@mfa.kfki.hu (Z. Osváth).

0.1–0.5 V. Atomic resolution images were achieved typically with $I_t=1$ nA and $U_t=0.1$ V.

3. Results and discussion

The STM investigation showed that the irradiation was successful in creating individual, atomic-scale nanotube defects (no similar defects could be detected on the as-grown nanotubes). Such a CNT defect is presented in Fig. 1(a) where the defect site appears as a protrusion (increased tunneling current) in the topographic STM image. Fig. 1(b) shows STS measurements performed above the defect site (continuous line) and above a defect-free region of the CNT (dashed line). The dI/dV curves—which are proportional to the local density of states (LDOS)—show that additional electronic states appear near the Fermi level at the defect site (the peak at ~ 0.1 eV).

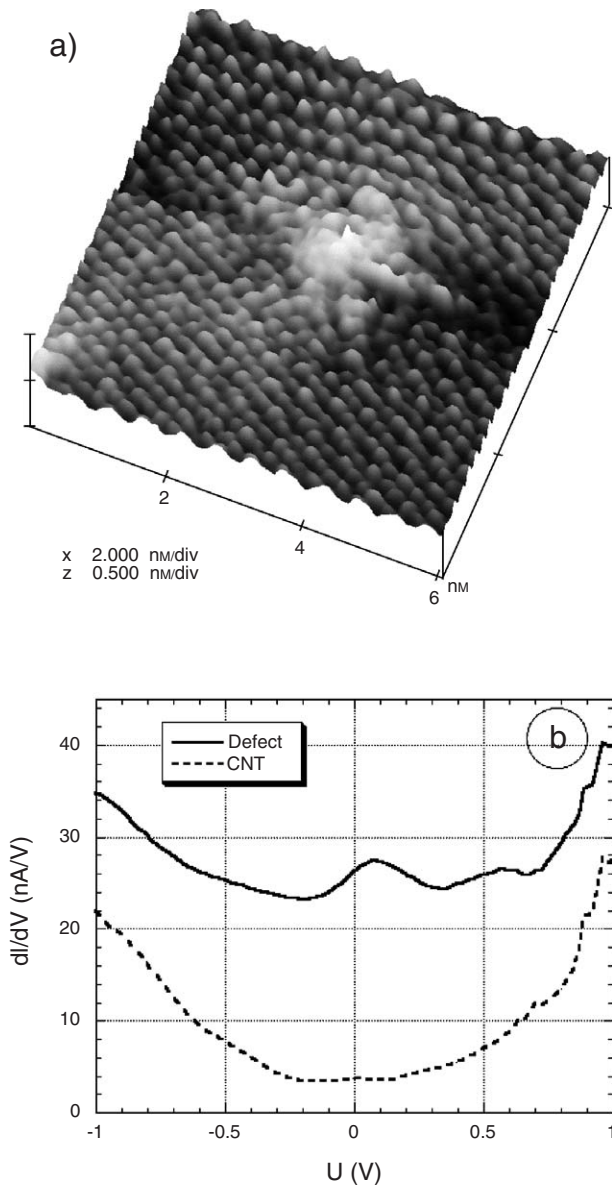


Fig. 1. (a) Atomic resolution STM image of a carbon nanotube defect produced by irradiation. (b) STS curves measured above the defect site (solid line) and above a defect-free portion of the nanotube (dashed line).

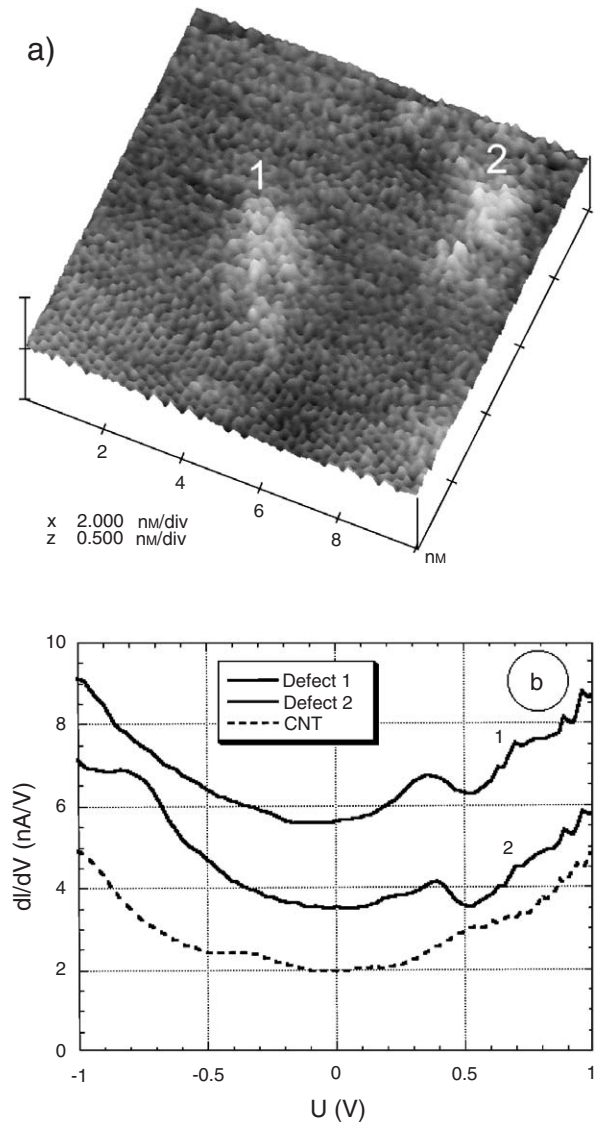


Fig. 2. (a) STM image of two nanotube defects recorded after the annealing of the irradiated sample. (b) dI/dV curves measured above the defects 1 and 2, respectively.

These additional states contribute to the tunneling process. As a result, when the scanning STM tip reaches the defect site the tunneling current increases compared to the current measured at the defect-free region. Consequently, the tip moves upwards on the z axis (0.1–0.2 nm farther from the CNT surface) in order to keep constant the value of I_t (constant current operating mode). This movement of the tip makes the “protrusion” of about 0.24 nm in height observed at the defect site in Fig. 1(a). The atomic resolution is lost at the defect site and one cannot directly determine which type of defect is observed (vacancy, non-hexagonal ring, etc.). These results are in agreement with the theoretical calculations, which predicted the STM signatures of atomic-scale CNT defects produced by ion irradiation [13–15]. In these calculations the protrusions occur due to the increased LDOS which stems from the dangling bonds produced by the incoming ions. Similar protrusions (hillocks) were observed earlier on irradiated HOPG surface [16,17].

As carbon nanotube defects can be annealed at high temperatures, we wanted to see the effect of such an annealing on the irradiated nanotubes. We heated the sample at 450 °C for 90 min under a nitrogen atmosphere of 5 bars. After annealing, further STM investigations were done under ambient conditions. The measurements revealed that the defects are still present in the nanotubes, however their measured heights are much lower. Fig. 2(a) shows two CNT defects measured after the annealing. The protrusions corresponding to these defects are less than 0.1 nm in height (the defect site labeled 1 in the image has an average height of 0.06 nm and the defect labeled 2 has 0.09 nm). The STS curves measured at these sites are shown in Fig. 2(b). Additional peaks are observed in these dI/dV data as well, but in this case they appear at higher energies (around 0.35 eV above the Fermi level). These results suggest that the nature of the defects changed during the annealing. Such kind of donor-like states can appear assuming that

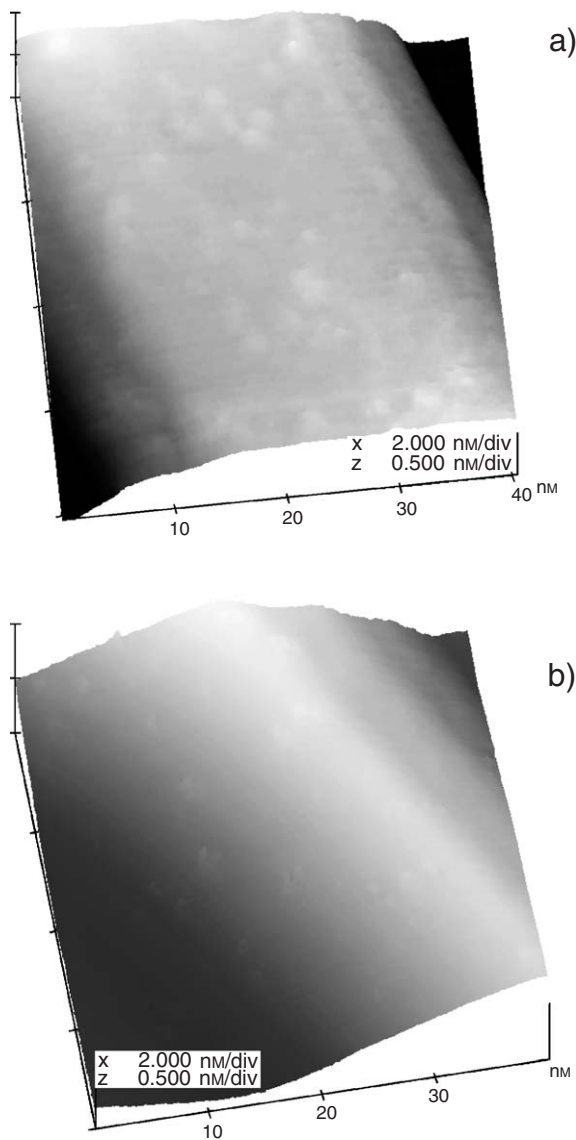


Fig. 3. 3D STM images of MWCNTs with irradiation-induced defects before (a) and after (b) annealing. After annealing the “heights” of the defects decrease.

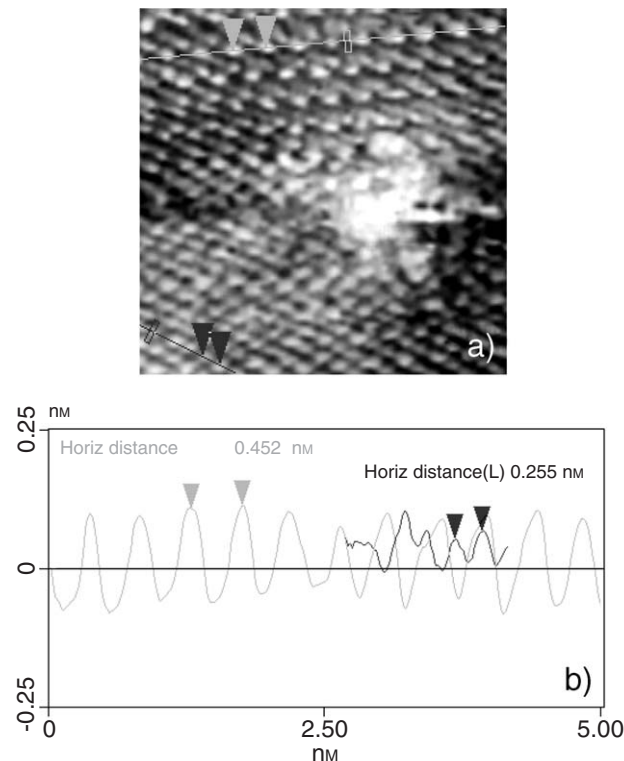


Fig. 4. $\sqrt{3}R \times \sqrt{3}R$ – type superstructures observed near the defect in (a). The cross sectional lines in (b) show the period determined by the atomic structure (black line) and the period of the superstructure (grey line).

nitrogen adsorbs at the defect sites [18,19]. Another possible mechanism is that during the annealing process the vacancy-type defects transformed into non-hexagonal ring-type defects by dangling bond saturation, predicted by molecular dynamical simulations [15]. Furthermore, the lower protrusions observed with STM after the heat treatment also show how CNT defects tend to heal already at moderate temperatures as compared with usual graphitization temperatures. This phenomenon can be well observed in Fig. 3. A CNT portion containing several defects is presented in Fig. 3(a). The protrusions corresponding to the defect sites are clearly visible in the image. On the other hand Fig. 3(b) shows a CNT portion after the heat treatment. One can observe that in this case—using the same tunneling conditions—the irradiation-induced hillocks were not very well observed. However, when scanning smaller areas ($10 \times 10 \text{ nm}^2$), the defect sites could be well distinguished again (see for example Fig. 2).

In the close vicinity of several defects we observed oscillations of the LDOS with a period larger than the period of the atomic structure. Such kind of oscillations (superstructures) can be observed in the top part of Fig. 4(a), near the defect site. The cross sectional lines in Fig. 4(b) show that the period of the observed superstructure is around 0.45 nm, while the period of the atomic structure is measured to be 0.255 nm. Such superstructures were observed earlier on HOPG surfaces [17,20] and were also predicted theoretically for single wall CNTs with vacancies [13]. They are known as $\sqrt{3}R \times \sqrt{3}R$ type superstructures [21,22], where $R=0.246 \text{ nm}$ is the

distance between B-site atoms in the HOPG. In our case $R=0.255$ nm and the period of the superstructure is approximately given by $\sqrt{3}$ times R . As pointed out in Ref. [22], these type of superstructures do not appear due to atomic rearrangement, but they are patterns formed by the interference of normal electron waves with electron waves scattered at the defect site.

4. Conclusions

Irradiated multi-wall carbon nanotubes were investigated by scanning tunneling microscopy and spectroscopy. In agreement with the theoretical expectations, the individual, atomic-scale CNT defects appeared as hillock-like protrusions in the STM images. These protrusions correspond to local tunneling current maxima caused by the changed electronic structure at the defect sites. After heating the sample at 450 °C, the protrusions measured at the defect sites decreased, which showed that the defects tend to heal already at moderate temperatures. Spectroscopic measurements also indicated that the nature of the defects had changed during the annealing process. We showed that electronic $\sqrt{3}R \times \sqrt{3}R$ -type superstructures, which had been observed earlier on HOPG surfaces, could also be detected near carbon nanotube defects.

Acknowledgement

This work has been done in the framework of the GDRE No. 2756 “Science and applications of the nanotubes—NANO-E”. The authors acknowledge the financial support of OTKA Grants T 43685 and T 43704 and of the “Nanotechnologia 2—NKFP 3A071_04” grant in Hungary.

References

- [1] M.S. Dresselhaus, G. Dresselhaus, P. Avouris, Carbon Nanotubes, Synthesis, Structure, Properties and Applications, Springer, Berlin, 2001.
- [2] V. Meunier, L. Henrard, Ph. Lambin, Phys. Rev., B 57 (1998) 2586.
- [3] F.L. Deepak, A. Govindaraj, C.N.R. Rao, Chem. Phys. Lett. 345 (2001) 5.
- [4] Z. Osváth, A.A. Koós, Z.E. Horváth, J. Gyulai, A.M. Benito, M.T. Martínez, W. Maser, L.P. Biró, Mater. Sci. Eng., C 23 (2003) 561.
- [5] J.W. Park, J. Kim, J.-O. Lee, K.C. Kang, J.-J. Kim, K.-H. Yoo, Appl. Phys. Lett. 80 (2002) 133.
- [6] P.M. Ajayan, V. Ravikumar, J.-C. Charlier, Phys. Rev. Lett. 81 (1998) 1437.
- [7] M.S. Raghuvver, P.G. Ganesan, J. D’Arcy-Gall, G. Ramanath, Appl. Phys. Lett. 84 (2004) 4484.
- [8] Y. Zhu, T. Yi, B. Zheng, L. Cao, Appl. Surf. Sci. 137 (1999) 83.
- [9] A.V. Krasheninnikov, K. Nordlund, Nucl. Instrum. Methods, B 216 (2004) 355.
- [10] A. Hashimoto, K. Suenaga, A. Glotter, K. Urita, S. Iijina, Nature 430 (2004) 870.
- [11] V. Meunier, Ph. Lambin, Carbon 38 (2000) 1729.
- [12] D. Orlikowski, M.B. Nardelli, J. Bernholc, C. Roland, Phys. Rev., B 61 (2000) 14194.
- [13] A.V. Krasheninnikov, Phys. Low-Dimens. Struct. 11/12 (2000) 1.
- [14] A.V. Krasheninnikov, K. Nordlund, M. Sirviö, E. Salonen, J. Keinonen, Phys. Rev., B 63 (2001) 245405.
- [15] A.V. Krasheninnikov, K. Nordlund, Sov. Phys. Solid State 44 (2002) 470.
- [16] L. Porte, M. Phaner, C.H. de Villeneuve, N. Moncoffre, J. Tousset, Nucl. Instrum. Methods, B 44 (1989) 116.
- [17] J.R. Hahn, H. Kang, Phys. Rev., B 60 (1999) 6007.
- [18] D. Srivastava, M. Menon, C. Daraio, S. Jin, B. Sadanadan, A.M. Rao, Phys. Rev., B 69 (2004) 153414.
- [19] A.H. Nevidomskyy, G. Csányi, M.C. Payne, Phys. Rev. Lett. 91 (2003) 105502.
- [20] L. Porte, C.H. de Villeneuve, M. Phaner, J. Vac. Sci. Technol., B 9 (1991) 1064.
- [21] H.A. Mizes, J.S. Foster, Science 244 (1989) 559.
- [22] G.M. Shedd, P.E. Russell, Surf. Sci. 266 (1992) 259.